

AD-A050 194

AERONAUTICAL RESEARCH COUNCIL LONDON (ENGLAND)  
THROUGH FLOW ANALYSIS OF VISCOUS AND TURBULENT FLOWS.(U)  
1978 A GOULAS, R C BAKER  
ARC-CP-1382

F/G 20/4

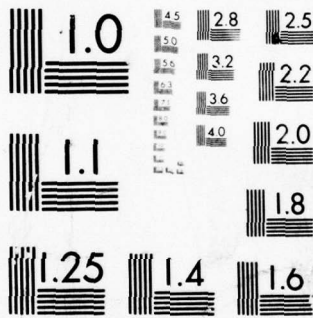
UNCLASSIFIED

NL

| OF |  
AD  
A050 194



END  
DATE  
FILMED  
3-78  
DDC



MICROCOPY RESOLUTION TEST CHART  
NATIONAL BUREAU OF STANDARDS-1963-A

C.P. No. 1382

AD A 050194

C.P. No. 1382

②

R



PROCUREMENT EXECUTIVE, MINISTRY OF DEFENCE

AERONAUTICAL RESEARCH COUNCIL

⑨ CURRENT PAPERS

AD No. DDC FILE COPY

⑥

Through Flow Analysis of Viscous and Turbulent Flows

⑭

ARC-CP-1382

⑫

30 p.

⑩

by  
Apostolos Goulas  
Roger C. Baker

⑪

1978

DDC  
RECEIVED  
FEB 21 1978  
REGISTRY  
A

LONDON: HER MAJESTY'S STATIONERY OFFICE

1978

008450

alt

THROUGH FLOW ANALYSIS OF  
VISCIOUS AND TURBULENT FLOWS

- by -

Apostolos Goulas  
and  
Roger C. Baker

SUMMARY

The matrix through-flow analysis is extended to cover turbulent and viscous flows by solving the streamwise equation of motion to obtain a suitable entropy field derived from the stresses.

The results of computation for straight circular pipe flows agree well with published data for laminar flow with and without swirl and for turbulent flow.

1. Introduction

Matrix through-flow analysis is widely used for calculation of the flow in turbomachines. It solves the equations of continuity, motion, energy and state. For inviscid fluids these equations are sufficient to determine the flow pattern. In order to simulate the flow of a viscous fluid, a loss model was introduced in the form of a local polytropic efficiency by Marsh<sup>10</sup>. The equations remained those of any inviscid flow.

Marsh and Bosman<sup>1</sup> derived equations which are consistent with the loss model, assuming that a dissipative force exists, which opposes the velocity vector. The loss model consists of either empirical data or equations relating the change of entropy to the fluid, the flow and the blade geometry.

The present paper is an attempt to connect the changes of the entropy both to the viscous terms of the Navier-Stokes equations and to the turbulence terms of the mean flow Navier-Stokes equations, and to deduce the flow of a viscous fluid without including empirical equations for the entropy. It is based on the analysis presented by Marsh and Bosman<sup>1</sup>.

2. Flow on a Mean Stream Surface

For a three-dimensional flow, the pattern can be found by solving the equations of

- (a) continuity
- (b) motion (3)
- (c) energy
- (d) state.

These six equations are sufficient to determine the fluid properties and the three components of velocity.

If the flow takes place on a prescribed stream surface, then there is a geometric condition relating the three components of velocity, which must be satisfied in order that the velocity vector lies on the stream surface. This geometric condition can replace one of the equations of motion in the solution for the flow pattern.

The replaced equation of motion can be used to evaluate the body force which must be applied for the flow to follow the prescribed stream surface.

If a rectangular co-ordinate system is chosen on the stream surface with axes S along and N across the stream, then the third axis, n, is normal to the surface (Fig.1).

The body force F, which is necessary for the inviscid flow to follow the stream surface, is normal to the surface. The equations of motion for the S and N directions therefore do not contain a component of F. These two equations are retained for calculating the flow pattern. The equation of motion for the n direction, which is replaced by the geometrical condition, contains the body force F and it can be used to determine the magnitude of this force.

For a reversible adiabatic flow on a prescribed stream surface, the flow pattern is determined by the following six equations

1. The continuity equation.

2a. The equation of motion for the N direction in a co-ordinate system rotating with the blade row

$$\bar{N} \cdot \bar{W} \times (\nabla \times \bar{V}) = \bar{N} \cdot (\nabla I - T \nabla S - \bar{D}) \quad (1)$$

or since  $\bar{N} \cdot \bar{D} = 0$

$$\bar{N} \cdot \bar{W} \times (\nabla \times \bar{V}) = \bar{N} \cdot (\nabla I - T \nabla S) \quad (2)$$

2b. The streamwise equation of motion

$$\bar{W} \cdot \bar{W} \times (\nabla \times \bar{V}) = \bar{W} \cdot (\nabla I - T \nabla S - \bar{D})$$

and using the energy equation for steady flow we get

$$T \frac{Ds}{Dt} = - \bar{W} \cdot \bar{D} \quad (3)$$

2c. A geometrical condition relating the three components of velocity expressed as

$$\bar{W} \cdot \bar{F} = 0 \quad (4)$$

3. Energy equation for steady flow

$$\frac{DI}{Dt} = 0 \quad (5)$$

assuming that it is valid for the individual streamlines in steady irreversible adiabatic flow.

4. The streamwise equation of motion which will be used to calculate the entropy field from the dissipation force  $\bar{D}$ . This is given by

$$\bar{D} = - \frac{1}{\rho} (\nabla \cdot \tau) \quad (6)$$

This is discussed in section 4.

This approach differs from the one by Marsh and Bosman who determine the entropy field from empirical data and use the streamwise equation of motion to calculate the dissipation force.

3. Analytical Equations

The treatment of the continuity equation, the equation of motion for the N direction and the geometric condition is the same as the one by Marsh and Bosman<sup>1</sup> (where the bar indicates special derivatives, so we will give here only the final equations.

3.1 Continuity

$$\frac{\bar{\partial}}{\partial r} (r B \rho V_r) + \frac{\bar{\partial}}{\partial z} (r B \rho V_z) = 0 \tag{7}$$

A stream function may then be defined as

$$\frac{\bar{\partial} \psi}{\partial r} = r B \rho V_z \tag{8a}$$

$$\frac{\bar{\partial} \psi}{\partial z} = -r B \rho V_r \tag{8b}$$

In this way the continuity equation is satisfied.

3.2 Geometric conditions

The velocity components are related by

$$W_r \tan \lambda + W_\theta + W_z \tan \mu = 0 \tag{9}$$

where by definition

$$\tan \lambda = \frac{n_r}{n_\theta} = \frac{F_r}{F_\theta} \tag{10a}$$

$$\tan \mu = \frac{n_z}{n_\theta} = \frac{F_z}{F_\theta} \tag{10b}$$

3.3 The N-direction equation of motion

This finally takes the form:

PROJECT NO.	
NTIS	WRITE SECTION <input checked="" type="checkbox"/>
DDI	DATE SECTION <input type="checkbox"/>
UNANNOUNCED	<input type="checkbox"/>
IDENTIFICATION	
BY	
DISTRIBUTION/AVAILABILITY CODES	
Dist.	AVAIL. IND./SPECIAL
A	

\* These are defined as

$$\frac{\bar{\partial} q}{\partial r} = \frac{\partial q}{\partial r} - \frac{n_r}{r n_u} \frac{\partial q}{\partial \theta} \qquad \frac{\bar{\partial} q}{\partial z} = \frac{\partial q}{\partial z} - \frac{n_z}{r n_u} \frac{\partial q}{\partial \theta}$$

and they represent the rate of change of a quantity q with r or z on a stream surface at a given value of z or r respectively.

$$\begin{aligned} \frac{\partial^2 \psi}{\partial r^2} + \frac{\partial^2 \psi}{\partial z^2} &= v_z \frac{\partial}{\partial r} (r B \rho) - v_r \frac{\partial}{\partial z} (r B \rho) + (r B \rho)^2 \frac{dI}{d\psi} - \\ &- \frac{r B \rho T}{w^2} \left[ \frac{\partial s}{\partial r} (v_z - w_\theta \tan \mu) - \frac{\partial s}{\partial z} (v_r - w_\theta \tan \lambda) \right] + \\ &+ \rho B \left[ \tan \mu \frac{\partial}{\partial r} (r v_\theta) - \tan \lambda \frac{\partial}{\partial z} (\rho v_\theta) \right] \end{aligned} \quad (11)$$

### 3.4 The S-direction equation of motion

This is given as

$$T \frac{Ds}{Dt} = - \bar{w} \cdot \bar{D} \quad (4)$$

where  $\bar{D}$  is the dissipation force and it is opposite to the velocity vector, then

$$\frac{D_r}{w_r} = \frac{D_\theta}{w_\theta} = \frac{D_z}{w_z} = K(w) \quad (12)$$

with  $K < 0$  and equation (3) becomes

$$T \frac{Ds}{Dt} = - w^2 K(w). \quad (13)$$

So the entropy increases along a streamline.

If the fluid is inviscid the dissipation force is zero, and equation (13) is reduced to  $s = \text{const}$  along streamlines.

### 4. The Dissipation Force

The dissipation force as shown in Appendix 1 is given as

$$\bar{D} = - \frac{1}{\rho} (\nabla \cdot \tau). \quad (6)$$

This can be calculated for every point in the field, provided that the viscosity is known.

Theoretically equation (12) will automatically be satisfied.

In practice this is not always true, because of

- (a) numerical errors involved in the calculation of the derivatives,
- (b) approximations involved in the calculation in the numerical value given for the viscosity.

In order to minimise the error the predominant components of the dissipation force and velocity are used to calculate the coefficient  $K(w)$ . This is expected to give very good results in cases where there is a predominant velocity but may cause problems in cases without it, e.g. recirculating flows.

5. The Solution of the Equations

This includes the following steps:

- (a) A distribution of the stream function  $\psi$  is assumed.
- (b) From equations (8) and (9) the three components of velocity can be calculated.
- (c) Then the stress components can be calculated from equations (12) and (8) respectively of Appendix 1.
- (d) The streamwise equation of motion is solved in order to get the entropy field as follows. (See Fig.2). Along a streamline equation (13) can be integrated,

$$\text{so } S_B = S_A - \int_A^B \frac{WK}{T} dL.$$

Assuming that  $WK$  is constant between  $A$  and  $B$ , we get

$$S_B = S_A - W \cdot K \cdot (AB)/T. \tag{14}$$

$S_A$  can be calculated as a function of the entropy of the neighbouring points and  $(AB)$  from the geometrical definition of the stream surface.

- (e) The right-hand side of equation (11) can be calculated and
- (f) a band matrix may be formed to solve equation (11).
- (g) The resulting  $\psi$  have to be compared with the initial  $\psi$ , and if the difference of the two  $\psi$  is greater than a certain acceptable value the whole procedure has to be repeated from the beginning.

6. The Flow in Axisymmetric Pipes

In order to check the whole procedure a computer program was written to calculate the flow in a straight circular pipe.

6.1 Equations of the flow

For axisymmetric flows

$$\frac{\partial}{\partial \theta} = 0. \tag{15}$$

The special derivatives are reduced to the usual partial derivatives.



If  $i, j, k$  are unit vectors in the  $r, \theta, z$  directions, the equations of motion can be expressed in the directions

$$j \times \bar{V}, \quad \bar{V} \times (j \times \bar{V}), \quad \bar{V}.$$

Again following the analysis by Bosman and Marsh<sup>1</sup> the equations will be

(a) Continuity

$$\frac{\partial}{\partial r} (r \rho V_r) + \frac{\partial}{\partial z} (r \rho V_z) = 0 \quad (16)$$

and a stream function is defined as

$$\frac{\partial \psi}{\partial r} = r \rho V_z \quad (17a)$$

$$\frac{\partial \psi}{\partial z} = -r \rho V_r \quad (17b)$$

(b) Equation of motion for  $j \times \bar{V}$  direction

$$\begin{aligned} \frac{\partial^2 \psi}{\partial r^2} + \frac{\partial^2 \psi}{\partial z^2} &= V_z \frac{\partial}{\partial r} (\rho r) - V_r \frac{\partial}{\partial z} (\rho r) + (\rho r)^2 \frac{d H_0}{d \psi} - \\ &- \frac{\rho r T}{V_m^2} \left[ V_z \frac{\partial s}{\partial r} - V_r \frac{\partial s}{\partial z} \right] - \\ &- \frac{\rho V_\theta}{V_m^2} \left[ V_z \frac{\partial}{\partial r} (r V_\theta) - V_r \frac{\partial}{\partial z} (r V_\theta) \right] \end{aligned} \quad (18)$$

(c) Equation of motion for  $\bar{V}$  direction

$$T \frac{Ds}{Dt} = -\bar{V} \cdot \bar{D} \quad (19)$$

(d) Equation of motion for  $\bar{V} \times (j \times \bar{V})$  direction

$$\frac{D}{Dt} (r V_\theta) = - \frac{r V_\theta}{V^2} \cdot T \cdot \frac{Ds}{Dt} \quad (20)$$

or taking into account equations (12) and (19) we get

$$\frac{D}{Dt} (r V_\theta) = r V_\theta \frac{Dz}{V_z} = r V_\theta K(V) \quad (21)$$

which shows that the angular momentum decreases in the direction of flow.

Equation (21) can be integrated along a streamline. The angular momentum at point B (Fig.2) can be expressed as

$$(r v_{\theta})_B = (r v_{\theta})_A e^{\int_A^B \frac{K}{v_m} dL} \quad (22)$$

Assuming that K is constant between A and B we get

$$(r v_{\theta})_B = (r v_{\theta})_A e^{\frac{K}{v_m} \int_A^B dL} \quad (23)$$

Equation (23) is of the same form as the equation derived by Talbot (13) for laminar swirling flows.

## 6.2 The computer program

This follows the steps described in section 5 with an extra calculation for the solution of the angular momentum equation (e.g. 23).

6.2.1 The finite difference.- Figs.3 to 5 give the lattices used for the finite difference, depending on the position of the point relative to the boundaries.

The derivatives are replaced with the following expressions

$$\frac{\partial \phi}{\partial x_j} = \sum a_{ij} \phi_i - \phi_0 \sum a_{ij} \quad \begin{array}{l} i = 1 \text{ to } 6 \\ j = r \text{ or } z \end{array} \quad (24)$$

and

$$\frac{\partial^2 \phi}{\partial r^2} + \frac{\partial^2 \phi}{\partial z^2} = \sum a_K \phi_i - \phi_0 \sum a_K \quad (25)$$

Coefficients  $a_{ij}$  or  $a_K$  are calculated using Taylor's series.

The error in the calculation of the derivatives is of the order

$$O \left[ \frac{\partial^4 \phi}{\partial x_j^4} \right]$$

6.2.2 The calculation of the flow conditions upstream of a point.- In order to solve equations (14) and (23) the conditions at the point A (Fig.2) have to be calculated. Normally point A does not coincide with a grid point so some approximations had to be made for the determination of

- (a) entropy at A
- (b) angular momentum
- and (c) distance AB.

For the entropy it was assumed that

$$S = S(\psi).$$

A cubic-spline polynomial was constructed to fit the entropy at  $i-1$  column and  $S_A$  was deduced from that polynomial.

The tangential velocity  $V_\theta$  was assumed to vary linearly between the points which include A.

The distance AB was approximated by a straight line between A and B.

The radius  $r_A$  was found again by cubic-spline polynomial fitting between radius  $r$  and stream function  $\psi$ .

## 7. Examples of the use of the Program

### 7.1 Laminar flow

7.1.1 Preservation of the profiles.- A fully developed two-dimensional laminar profile was set as the initial profile at the entry of the pipe.

7.1.1.1 Initial conditions.- The velocity is given by the relation

$$V_z = 2 V_o \left( 1 - \frac{r^2}{a^2} \right) \quad (26a)$$

and 
$$V_r = 0. \quad (26b)$$

Substituting e.g. (26a) to (17a) we get

$$\frac{\partial \psi}{\partial r} = 2 r \rho V_o \left( 1 - \frac{r^2}{a^2} \right) \quad (27)$$

which can be integrated along the entrance of the pipe with the boundary condition

$$\psi = 0 \quad \text{at} \quad r = 0$$

to give

$$\psi = 2 \rho V_o \left( \frac{r^3}{2} - \frac{r^4}{4a^2} \right) \quad (28)$$

Assuming that the total enthalpy  $H_o$  is constant at the entry,

$$\frac{d H_o}{d \psi} = 0, \quad (29)$$

we get equation (18)

$$\rho V_z + r \rho \frac{\partial V_z}{\partial r} = \rho V_z - \frac{r \rho T}{V_z^2} V_z \frac{\partial s}{\partial r}$$

or

$$\frac{\partial s}{\partial r} = - \frac{1}{T} \frac{\partial}{\partial r} \left( \frac{V_z^2}{2} \right) \quad (30)$$

and assuming that

$$s = 0, \quad V_z = 2 V_o \quad \text{at} \quad r = 0$$

we get

$$s(r,0) = \frac{1}{2T} \left( 4 V_0^2 - V_z^2 \right) \quad (31)$$

7.1.1.2 Boundary conditions.- Table 1 gives the boundary conditions applied.

Table 1

Boundary conditions for the developed laminar velocity profile

Quantity	Value on the axis	Value at the wall
Stream function $\psi$	$\psi = \text{const.}$	$\psi = \text{const.}$
Axial velocity $V_z$	$2 V_0$	0
Radial velocity $V_r$	0	0
$\tau_{rz}$	0	$2 \rho V_{zW} \nu a / (r_w^2 - a^2)$
$\tau_{zz}$	0	0

It was assumed that the velocity near the wall has a parabolic distribution, as a result of which the stress component  $\tau_{rz}$  is given by the relation

$$\tau_{rz} = 2 \rho V_{zW} \nu a / (r^2 - a^2).$$

The entropy increase along the wall is proportional to the dissipation force of the nearest internal point or

$$S_B = S_A - D_z (\Delta z) / T$$

7.1.1.3. Exit conditions.- It was assumed that  $V_r = 0$  which in turn means that

$$\frac{\partial \psi}{\partial z} = 0$$

It is assumed that entropy varies linearly with distance z.

7.1.1.4. The results.- Fig.6 gives the calculated profiles and the analytical ones.

For a distance of 20 diameters the velocity profile changes by about 2.5% of the analytical value.

This deviation can be attributed to the fact that the order of magnitude of the error of the finite difference approximation is  $O \left[ \frac{\partial^4 \psi}{\partial r^4} \right]$  and this is not zero as can be seen from equation (28).

7.1.2 The development of laminar flow.- An initial uniform velocity profile was set at the entry of the pipe and the development of the flow profile was predicted.

7.1.2.1 Initial conditions.- The distribution of velocity across the entrance is

$$V_z = V_0 \quad (32a)$$

$$V_r = 0 \quad (32b)$$

Substituting equation (32a) into (17a) we get

$$\frac{\partial \psi}{\partial r} = r \rho V_0 \quad (33)$$

The above equation can be integrated along the entrance of the pipe with the boundary condition  $\psi = 0$  at  $r = 0$

to give

$$\psi = \rho V_0 \frac{r^2}{2} \quad (34)$$

Across the entrance of the pipe we again take

$$H_0 = \text{const.}$$

and for the entropy

$$S(r,0) = 0.$$

7.1.2.2 Boundary conditions.- Table 2 gives the boundary conditions applied.

It is assumed again that the velocity near the wall has a parabolic distribution.

Table 2

Boundary conditions for the development of laminar flow

Quantity	Value on the axis	Value at the wall
Stream function $\psi$	$\psi = \text{const.}$	$\psi = \text{const.}$
Axial velocity $V_z$	$\frac{\partial V_z}{\partial r} = 0$	0
Radial velocity $V_r$	0	0
$\tau_{rz}$	0	$2 V_{zW} \nu a / (r_w^2 - a^2)$
$\tau_{zz}$	$\frac{\nu V_z (I+1) - V_z(I)}{\rho \Delta z}$	0
Increase of entropy	0	$\frac{\Delta \tau_{rz}}{\Delta r} + \frac{\tau_{rzW}}{a}$

7.1.2.4 The results.- Fig.7 gives the calculated axial velocity profiles at different distances from the entry, with the corresponding experimental profiles by Nikuradze in Schlichting<sup>12</sup>.

There is a discrepancy of about 6% for the values of the velocity at a distance of 5 diameters which is reduced gradually to almost zero at distances higher than 25 diameters. We think that this is due to the inaccuracy of calculating the shear stresses near the wall at the first few stations downstream of the entrance of the pipe.

Nevertheless, the values of the velocity at the centreline are identical with those calculated by Boussinesq as they are given by Schlichting<sup>12</sup> on the graph with Nikuradze's data.

7.1.3 Effect of swirl on fully developed laminar flow.- A tangential velocity is superimposed on a fully developed laminar flow at the entry of a pipe, and the development of the flow profile is given.

7.1.3.1 Initial conditions.- The axial velocity is given by the relation

$$V_z = 2 V_0 \left( 1 - \frac{r^2}{a^2} \right) \tag{35a}$$

$$V_r = 0 \tag{35b}$$

$$V_\theta = \omega r \tag{35c}$$

The stream function distribution is given by the relation

$$\psi = 2 \rho V_0 \left( \frac{r^2}{2} - \frac{r^4}{4a^2} \right) \tag{28}$$

The total enthalpy is

$$H_0 = \text{const.}$$

and the distribution of entropy is

$$s(r,0) = \frac{1}{T} \left[ 4 V_0^2 \frac{r^2}{a^2} \left( 1 - \frac{r^2}{2a^2} \right) - \omega^2 r^2 \right] \tag{29}$$

7.1.3.2 Boundary and exit conditions.- These are the same as for the fully developed laminar flow, except that at the axis we now have

$$\frac{\partial V_z}{\partial r} = 0$$

or the axial velocity at the centreline is equal to the velocity at the nearest point with the same z.

7.1.3.3 The results.- Fig.8 gives the axial velocity profile for an initial swirl  $\omega = 4$  at a distance of 5 diameters from the entry of the pipe.

At the axis the velocity is reduced and the velocity towards the pipe wall is increased.

Similar behaviour is shown theoretically by Talbot<sup>13</sup>, although he predicts smaller values for the velocity at the centreline.

Fig.9 gives the flow profiles for a distance of 25 diameters and for  $\omega = 4$ .

The axial velocity profile becomes flatter at the centreline as the angular velocity increases.

For values of  $\omega a/V_0 > 1$  for Re between 20 and 2000 the computer program breaks down. This is due to the fact that during the computation reverse flow appears at the axis which moves towards the entry from iteration to iteration. The program breaks when the reverse region reaches the entry, because a discontinuity of velocity appears at the entry with which the initial conditions cannot cope.

Fig.10 shows the decay of the tangential velocity profile. The profiles are similar for different  $\omega$ , or the ratio

$$V_{\theta}/\omega a$$

is independent of the angular velocity  $\omega$ .

The profiles are similar to those given by Lavan et al<sup>3</sup>.

Fig.11 gives the distribution of the radial velocity at a distance of 8 diameters from the entry, for 3 angular velocities. The profiles are similar to those given by Talbot<sup>13</sup>.

## 7.2 Turbulent flow

The equations of motion as described in vector form by equation (1) or in analytical form in Appendix 1, remain the same for the mean velocities. The only difference is that the dissipation force now contains derivatives of the Reynolds stresses due to turbulence, and an extra problem appears, namely, how to calculate these extra stresses.

One basic assumption made by those who have used numerical models for turbulence is that the turbulence is isotropic. Hence it follows that there is a scalar turbulent viscosity  $\mu_t$  which satisfies the relation

$$-\rho \overline{u_i u_j} = \mu_t \left[ \frac{\partial U_i}{\partial x_j} + \frac{\partial U_j}{\partial x_i} \right] \quad (36)$$

and also links the stresses due to turbulence with the mean velocity gradients of the flow at each point.

For the pipe flow an initial mean velocity distribution is assumed

$$V_z = V_{om} \left( \frac{a-r}{a} \right)^{1/9} \quad (37)$$

The distribution of the stream function across the entrance of the pipe will be

$$\psi = \rho \frac{9V_{om}}{a^{1/9}} \left[ \frac{(a-r)^{10/9}}{19} - \frac{a}{10} (a-r)^{1/9} + \frac{9a^{10/9}}{190} \right] \quad (38)$$

the boundary condition for  $\psi$  being that

$$\psi = 0 \quad \text{at} \quad r = 0 \quad \text{and} \quad z = 0.$$

The initial distribution of entropy is given by equation (31)

$$s(r,0) = \frac{1}{2T} \left( V_{om}^2 - V_z^2 \right). \quad (39)$$

The boundary conditions and the exit conditions are the same as for the fully developed laminar flow, with the exception of the stress  $\tau_{rz}$  at the wall.



7.2.1 Solution with given  $\mu_t$ .- As a first step towards a solution of the turbulent flow in a pipe, the distribution of the turbulent viscosity was taken as

$$\mu_t = c a u^* \quad (40)$$

where  $c$  takes the following values

$$c = 0.07 (a - r)/a \quad \text{for} \quad 0 < a - r < 0.25 a \quad (41a)$$

and  $c = 0.07 \quad \text{for} \quad 0.25 a < a - r < a \quad (41b)$

$$u^* = 0.035 V_{0m}$$

These were taken from Hinze<sup>9</sup> based on data by Laufer for  $Re = 50\,000$ . The wall shear stress is

$$\tau_{rz} = \rho u^{*2} \quad (42)$$

7.2.1.1 Results.- Fig.12 gives the profile of the axial velocity across the entrance of the pipe and also after a distance of 6 diameters.

The maximum deviation is of the order of 0.4%.

7.2.2 The  $K - \epsilon$  model for turbulence.- A more elaborate model for turbulence is the  $K - \epsilon$  model proposed first by Harlow and Nakayama<sup>8</sup>.

Hanjalic<sup>6</sup> developed two transport equations, one for the kinetic energy of turbulence  $K$ , and one for the rate of dissipation of turbulence.

In cylindrical co-ordinates for axisymmetric flow and for high Reynolds numbers the equations are:

$$\frac{D\epsilon}{Dt} = \frac{1}{\rho} \left[ \frac{1}{r} \frac{\partial}{\partial r} \left( \frac{\mu_t r}{\sigma_\epsilon} \frac{\partial \epsilon}{\partial r} \right) + \frac{\partial}{\partial z} \left( \frac{\mu_t}{\sigma_\epsilon} \frac{\partial \epsilon}{\partial z} \right) \right] + c_1 \frac{\mu_t \epsilon}{\rho K} G - c_2 \frac{\epsilon^2}{K} \quad (43a)$$

$$\frac{DK}{Dt} = \frac{1}{\rho} \left[ \frac{1}{r} \frac{\partial}{\partial r} \left( \frac{\mu_t r}{\sigma_K} \frac{\partial K}{\partial r} \right) + \frac{\partial}{\partial z} \left( \frac{\mu_t}{\sigma_K} \frac{\partial K}{\partial z} \right) \right] + \frac{\mu_t}{\rho} G - \epsilon \quad (43b)$$

where

$$G = 2 \left[ \left( \frac{\partial v_z}{\partial z} \right)^2 + \left( \frac{\partial v_r}{\partial r} \right)^2 \right] + \left( \frac{\partial v_z}{\partial r} + \frac{\partial v_r}{\partial z} \right)^2 + 2 \left( \frac{v_r}{r} \right)^2 + \left( \frac{\partial v_u}{\partial r} \right)^2 + \left( \frac{\partial v_u}{\partial z} \right)^2 \quad (44)$$

and the turbulence viscosity will be

$$\mu_t = c_\mu \rho K^2 / \epsilon \quad (45)$$

The various constants appearing in these equations, as given by Launder and Spalding<sup>4</sup>, are

$$\begin{aligned} c_{\mu} &= 0.09, & c_1 &= 1.44, & c_2 &= 1.92 \\ \sigma_K &= 1, & \sigma &= 1.3, & c_D &= 0.08. \end{aligned}$$

Equations (43a) and (43b) have to be solved for each iteration of the stream function.

The initial conditions are

$$K = \ell^2 \left( \frac{\partial V_z}{\partial r} \right)^2 / \sqrt{c_D}$$

$$\varepsilon = c_D^{0.75} K^{1.5} / \ell$$

taken from Launder and Spalding<sup>5</sup>.

For points near the wall it is assumed that the velocity profile follows the logarithmic law,

$$\frac{V_{z_w}}{u_T} = \frac{1}{0.41} \ell \eta \left[ 9 u_T (a - r_w) \rho / \mu \right]$$

Then the kinetic energy of turbulence will be

$$K_w = u_T^2 / 0.3$$

and the rate of dissipation will be

$$\varepsilon_w = \frac{c_D^{0.75}}{\mu} K^{1.5} / [0.41 (a - r_w)].$$

7.2.2.1 Results.- The initial mean velocity profile does not change along the pipe by more than -0.3% for a distance of 6 diameters downstream of the entrance.

## 8. Conclusions

A new approach to the use of the dissipation force in through-flow analysis is discussed which permits more accurate calculation of a flow field when no data for the entropy exists.

The dissipation force is calculated taking into account the viscous and turbulence terms of the Navier-Stokes equations.

A computer program was written and different cases of pipe flow were checked.

The fully developed laminar flow profile remains unchanged to within 2.5% for a distance of 20 diameters.

The development of the laminar flow is predicted satisfactorily.

The effect of swirl on fully developed laminar flows is predicted, but because of lack of suitable experimental data it has not been possible to compare the results with experiments.

In the case of turbulent flow, two models for the Reynolds stresses were used, both with very satisfactory results.

Acknowledgements

The authors are indebted to Prof. H. Marsh, both for suggesting that the method could be tested on pipe flows and also for several valuable discussions.

Nomenclature

B	integration factor for the continuity equation
D	dissipation force per unit mass
F	body force per unit mass
h	enthalpy
H <sub>0</sub>	stagnation enthalpy
I	rothalpy, $I = H_0 - \omega rV_\theta$
K	ratio of dissipation force to velocity
K	kinetic energy of turbulence
n	normal to stream surface
N	normal to streamline
r	radius
s	entropy
S	streamwise direction
T	temperature
$\bar{V}$	velocity vector
$\bar{W}$	relative velocity vector
z	axial direction
$\theta$	circumferential direction
$\lambda, \mu$	angles defined by equations (10)
$\omega$	angular velocity
$\tau$	stress tensor
L	distance along a streamline
$\ell$	length scale of turbulence
V <sub>m</sub>	meridional velocity

$\psi$	stream function
$a$	coefficients for the calculation of the derivatives
$V_0$	mean velocity of the laminar flow
$a$	radius of the pipe
$\nu$	kinematic viscosity
$\phi$	a representative variable
Re	Reynolds number, $Re = \frac{dV_0}{\nu}$
$V_{om}$	maximum velocity at the axis for turbulent flow
$\mu_t$	turbulent viscosity
$\epsilon$	rate of dissipation of turbulence energy
$x_i$	Cartesian space co-ordinate

Subscripts

$w$	point near the wall
CL	point on the axis
$i, j, k$	subscripts denoting Cartesian co-ordinate directions.

---

References

<u>No</u>	<u>Author(s)</u>	<u>Title, Date, etc.</u>
1	C. Bosman and H. Marsh	An improved method for calculating the flow in turbomachines including a consistent loss model. Journal of Mech. Eng. Sci., Vol.16, No.4. 1974.
2	J.H. Horlock	On entropy production in adiabatic flow in turbomachines. J. Basic Engg., Trans. ASME Series D, Vol.93, pp.587-593. 1971.
3	Z. Lavan, H. Nielson and A.A. Fejer	Separation and flow reversal in swirling flows in circular ducts. Physics of Fluids, Vol.12, No.9. 1959.
4	B.E. Launder and D.B. Spalding	The numerical computation of turbulent flows. Computer methods in Applied Mech. Engg. 3. 1974.
5	B.E. Launder and D.B. Spalding	Mathematical models of turbulence. Academic Press, London. 1972.
6	K. Hanjalic	Two-dimensional asymmetric turbulent flow in ducts. Ph.D. thesis, University of London. 1970.
7	K. Hanjalic and B.E. Launder	A Reynolds-stress model of turbulence and its application to asymmetric shear flows. J. Fluid Mech., 52, pp.609-638. 1972.
8	F.H. Harlow and P. Nakayama	Transport of turbulence energy decay rate. Los Alamos Science Lab., University of California, Report LA-3854. 1968.
9	J.O. Hinze	Turbulence. McGraw-Hill, Second Edition. 1975.
10	H. Marsh	A digital computer programme for the through flow fluid mechanics in an arbitrary turbomachine using a matrix method. ARC R&M No.3509. 1968.
11	T.H. Moulden and J.M. Wu	An outline of methods applicable to viscous fluid flow problems. Army Missile Command, Redstone, RE-TR-71-4. 1971.
12	H. Schlichting	Boundary layer theory. McGraw-Hill, 6th edition. 1968.
13	L. Talbot	Laminar swirling pipe flow. Journal of Applied Mechanics, Vol.21, p.4. 1954.
14	C.H. Wu	A general theory of three-dimensional flow in subsonic and supersonic turbomachines of axial, radial and mixed flow types. NACA TN-2604. 1952.

Appendix 1

The Calculation of the Dissipation Force

1. The Navier-Stokes Equations

The momentum equations in cylindrical co-ordinates are given by Moulden and Wu<sup>11</sup> for steady flows

$$v_r \frac{\partial v_r}{\partial r} + \frac{v_\theta}{r} \frac{\partial v_r}{\partial \theta} + v_z \frac{\partial v_r}{\partial z} - \frac{v_\theta^2}{r} = - \frac{1}{\rho} \frac{\partial p}{\partial r} + \frac{1}{\rho} (\nabla \cdot \tau)_r \quad (A1a)$$

$$v_r \frac{\partial v_\theta}{\partial r} + \frac{v_\theta}{r} \frac{\partial v_\theta}{\partial \theta} + v_z \frac{\partial v_\theta}{\partial z} + \frac{v_\theta v_r}{r} = - \frac{1}{r\rho} \frac{\partial p}{\partial \theta} + \frac{1}{\rho} (\nabla \cdot \tau)_\theta \quad (A1b)$$

$$v_r \frac{\partial v_z}{\partial r} + \frac{v_\theta}{r} \frac{\partial v_z}{\partial \theta} + v_z \frac{\partial v_z}{\partial z} = - \frac{1}{\rho} \frac{\partial p}{\partial z} + \frac{1}{\rho} (\nabla \cdot \tau)_z \quad (A1c)$$

Using the relations

$$I = H_0 - \omega r v_\theta = h + \frac{1}{2} v^2 - \omega r v_\theta \quad (A2)$$

and 
$$\nabla h = T \nabla s + \frac{1}{\rho} \nabla p$$

we get

$$\frac{1}{\rho} \nabla p = \nabla I - T \nabla s - \frac{1}{2} \nabla v^2 + \omega \nabla (r v_\theta) \quad (A3)$$

Equations (A1) will become

$$\begin{aligned} \frac{v_\theta}{r} \left[ \frac{\partial}{\partial r} (r v_\theta) - \frac{\partial v_r}{\partial \theta} \right] - v_z \left[ \frac{\partial v_r}{\partial z} - \frac{\partial v_z}{\partial r} \right] &= \\ &= \frac{\partial I}{\partial r} - T \frac{\partial s}{\partial r} - \frac{1}{\rho} (\nabla \cdot \tau)_r \end{aligned} \quad (A4a)$$

$$\begin{aligned} \frac{v_r}{r} \left[ \frac{\partial}{\partial r} (r v_\theta) - \frac{\partial v_r}{\partial \theta} \right] - \frac{v_z}{r} \left[ \frac{\partial v_z}{\partial \theta} - \frac{\partial}{\partial z} (r v_\theta) \right] &= \\ &= \frac{1}{r} \frac{\partial I}{\partial \theta} - \frac{T}{r} \frac{\partial s}{\partial \theta} - \frac{1}{\rho} (\nabla \cdot \tau)_\theta \end{aligned} \quad (A4b)$$

and

$$\begin{aligned} \frac{v_r}{r} \left[ \frac{\partial v_r}{\partial z} - \frac{\partial v_z}{\partial r} \right] - \frac{w_\theta}{r} \left[ \frac{\partial v_z}{\partial \theta} - \frac{\partial}{\partial z} (r v_\theta) \right] &= \\ &= \frac{\partial I}{\partial z} - T \frac{\partial s}{\partial z} - \frac{1}{\rho} (\nabla \cdot \tau)_z \end{aligned} \quad (A4c)$$

The equations of motion as used by Bosman and Marsh<sup>1</sup> are

$$\begin{aligned} \frac{w_\theta}{r} \left[ \frac{\partial}{\partial r} (r v_\theta) - \frac{\partial v_r}{\partial \theta} \right] - v_z \left[ \frac{\partial v_r}{\partial z} - \frac{\partial v_z}{\partial r} \right] &= \\ &= \frac{\partial I}{\partial r} - T \frac{\partial s}{\partial r} - D_r \end{aligned} \quad (A5a)$$

$$\begin{aligned} - \frac{v_r}{r} \left[ \frac{\partial}{\partial r} (r v_\theta) - \frac{\partial v_r}{\partial \theta} \right] + \frac{v_z}{r} \left[ \frac{\partial v_z}{\partial \theta} - \frac{\partial}{\partial z} (r v_\theta) \right] &= \\ &= \frac{1}{r} \frac{\partial I}{\partial \theta} - \frac{T}{r} \frac{\partial s}{\partial \theta} - D_\theta \end{aligned} \quad (A5b)$$

$$\begin{aligned} \frac{v_r}{r} \left[ \frac{\partial v_r}{\partial z} - \frac{\partial v_z}{\partial r} \right] - \frac{w_\theta}{r} \left[ \frac{\partial v_z}{\partial \theta} - \frac{\partial}{\partial r} (r v_\theta) \right] &= \\ &= \frac{\partial I}{\partial z} - T \frac{\partial s}{\partial z} - D_z \end{aligned} \quad (A5c)$$

Comparing equations (A4) and (A5) we get

$$\frac{1}{\rho} (\nabla \cdot \tau)_r = D_r \quad (A6a)$$

$$\frac{1}{\rho} (\nabla \cdot \tau)_\theta = D_\theta \quad (A6b)$$

$$\frac{1}{\rho} (\nabla \cdot \tau)_z = D_z \quad (A6c)$$

or in a vector form

$$\bar{D} = \frac{1}{\rho} (\nabla \cdot \tau) \quad (A7)$$

2. The Components of the Stress Tensor

According to Moulden and Wu<sup>10</sup> the expression  $(\nabla \cdot \tau)$  is given by the following relations:

$$(\nabla \cdot \tau)_r = \frac{\partial}{\partial z} \tau_{zr} + \frac{1}{r} \frac{\partial}{\partial \theta} \tau_{r\theta} + \frac{\partial}{\partial r} \tau_{rr} + \frac{\tau_{rr} - \tau_{\theta\theta}}{r} \quad (\text{A8a})$$

$$(\nabla \cdot \tau)_\theta = \frac{\partial}{\partial z} \tau_{z\theta} + \frac{1}{r} \frac{\partial}{\partial \theta} \tau_{\theta\theta} + \frac{\partial}{\partial r} \tau_{r\theta} + 2 \frac{\tau_{r\theta}}{r} \quad (\text{A8b})$$

$$(\nabla \cdot \tau)_z = \frac{\partial}{\partial z} \tau_{zz} + \frac{1}{r} \frac{\partial}{\partial \theta} \tau_{z\theta} + \frac{\partial}{\partial r} \tau_{rz} + \frac{\tau_{rz}}{r} \quad (\text{A8c})$$

The strain tensor is given by the relations

$$\frac{1}{2} e_{rr} = \frac{\partial V_r}{\partial r} \quad (\text{A9a})$$

$$\frac{1}{2} e_{\theta\theta} = \frac{1}{r} \frac{\partial W_\theta}{\partial \theta} + \frac{V_r}{r} \quad (\text{A10b})$$

$$\frac{1}{2} e_{zz} = \frac{\partial V_z}{\partial z} \quad (\text{A10c})$$

$$e_{z\theta} = \frac{\partial W_\theta}{\partial z} + \frac{1}{r} \frac{\partial V_z}{\partial \theta} \quad (\text{A11a})$$

$$e_{zr} = \frac{\partial V_z}{\partial r} + \frac{\partial V_r}{\partial z} \quad (\text{A11b})$$

$$e_{r\theta} = \frac{1}{r} \frac{\partial V_r}{\partial \theta} + \frac{\partial W_\theta}{\partial r} - \frac{W_\theta}{r} \quad (\text{A11c})$$

For fluids which follow Stokes' law the stresses are given by the following relations

$$\tau_{rr} = - \frac{2}{3} \mu (\nabla \cdot \vec{v}) + \mu e_{rr} \quad (\text{A12a})$$

$$\tau_{\theta\theta} = - \frac{2}{3} \mu (\nabla \cdot \vec{v}) + \mu e_{\theta\theta} \quad (\text{A12b})$$

$$\tau_{zz} = - \frac{2}{3} \mu (\nabla \cdot \vec{v}) + \mu e_{zz} \quad (\text{A12c})$$



$$\tau_{rz} = \tau_{zr} = \mu e_{zr} \quad (A12d)$$

$$\tau_{z\theta} = \tau_{\theta z} = \mu e_{\theta z} \quad (A12e)$$

$$\tau_{r\theta} = \tau_{\theta r} = \mu e_{\theta r} \quad (A12f)$$

where the divergence of the velocity vector

$$\nabla \cdot \bar{v} = \frac{\partial v_z}{\partial z} + \frac{1}{r} \frac{\partial w_\theta}{\partial \theta} + \frac{\partial v_r}{\partial r} + \frac{v_r}{r} \quad (A13)$$

For incompressible fluids the divergence of the velocity can be set equal to zero from the continuity equation.

So if  $\rho = \text{const.}$

$$\nabla \cdot \bar{v} = 0 \quad (A14)$$

BMG

at the point  
of the  
flow

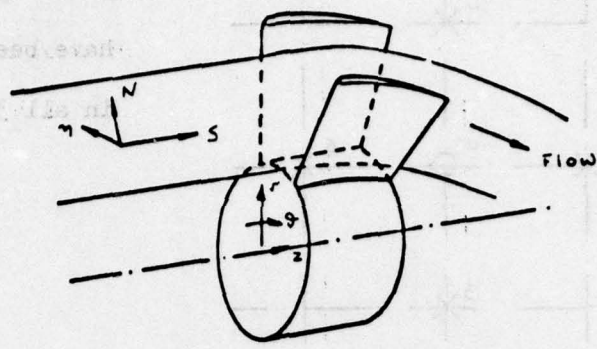


Figure 1. See Section 2.

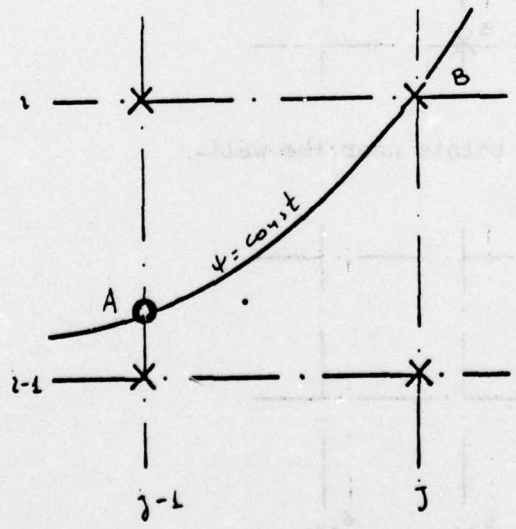
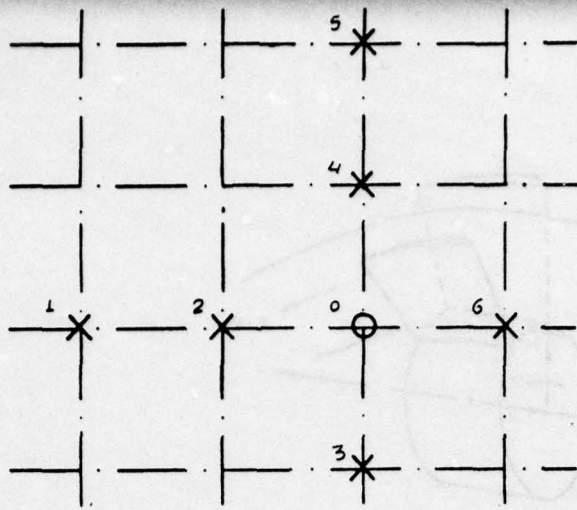


Figure 2. See Section 5.



Lattice points  
have been numbered  
in all 3 figures.

Fig. 3. Main Lattice.

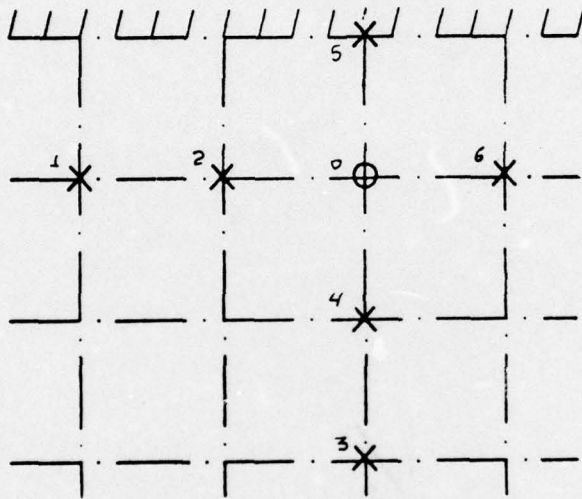


Fig. 4. Lattice for points near the wall.

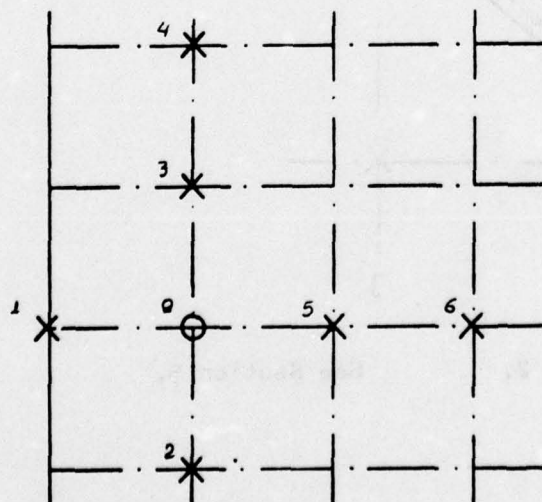


Fig. 5. Lattice at the entry.

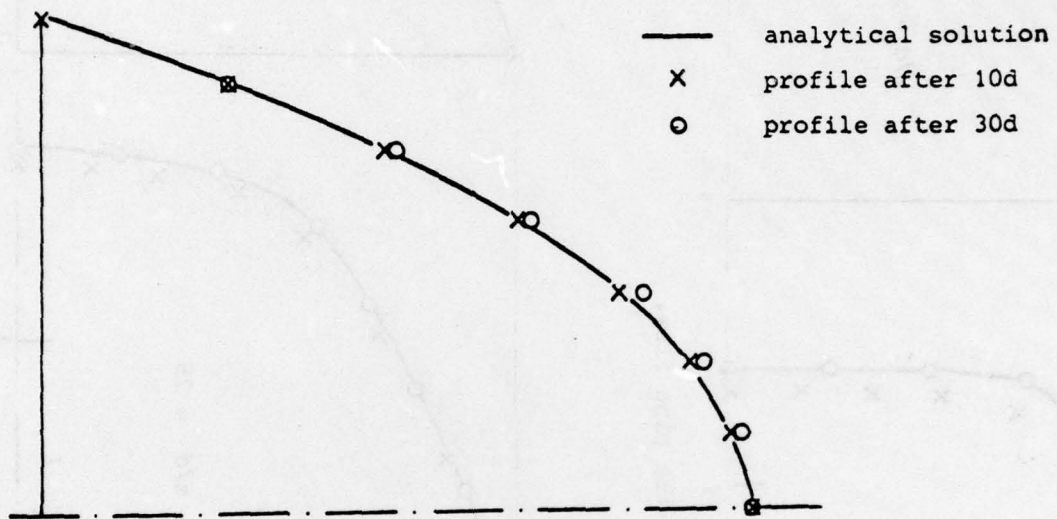


Fig. 6. Laminar flow profile.

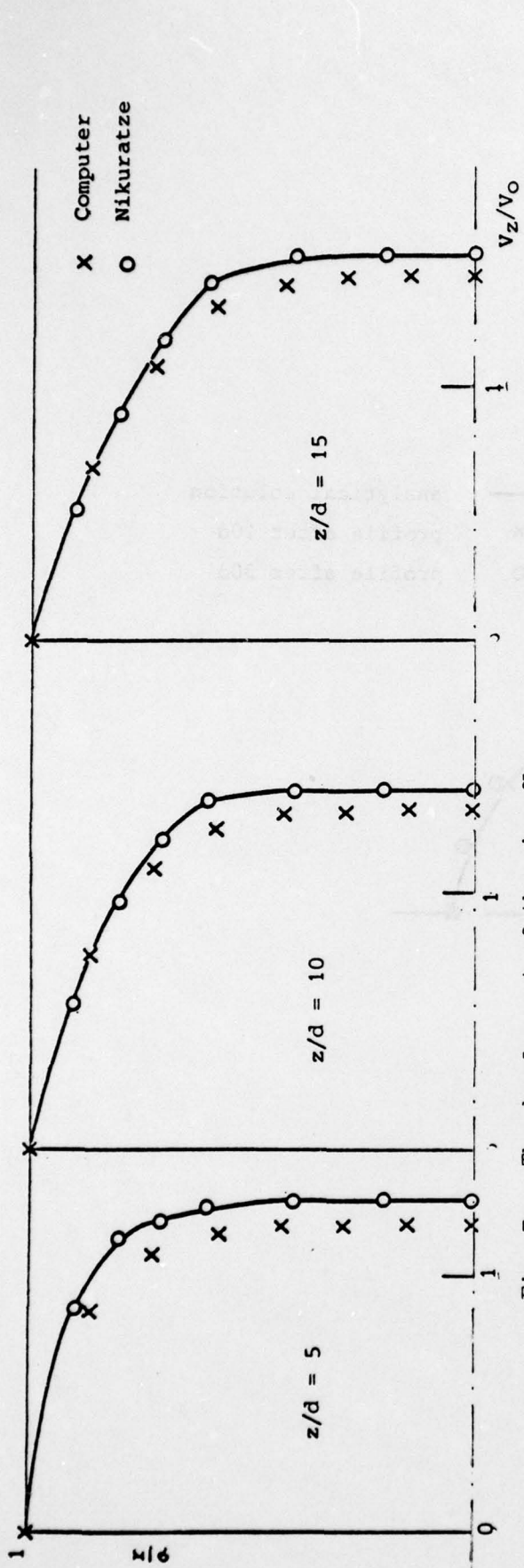


Fig. 7a. The development of the pipe flow.

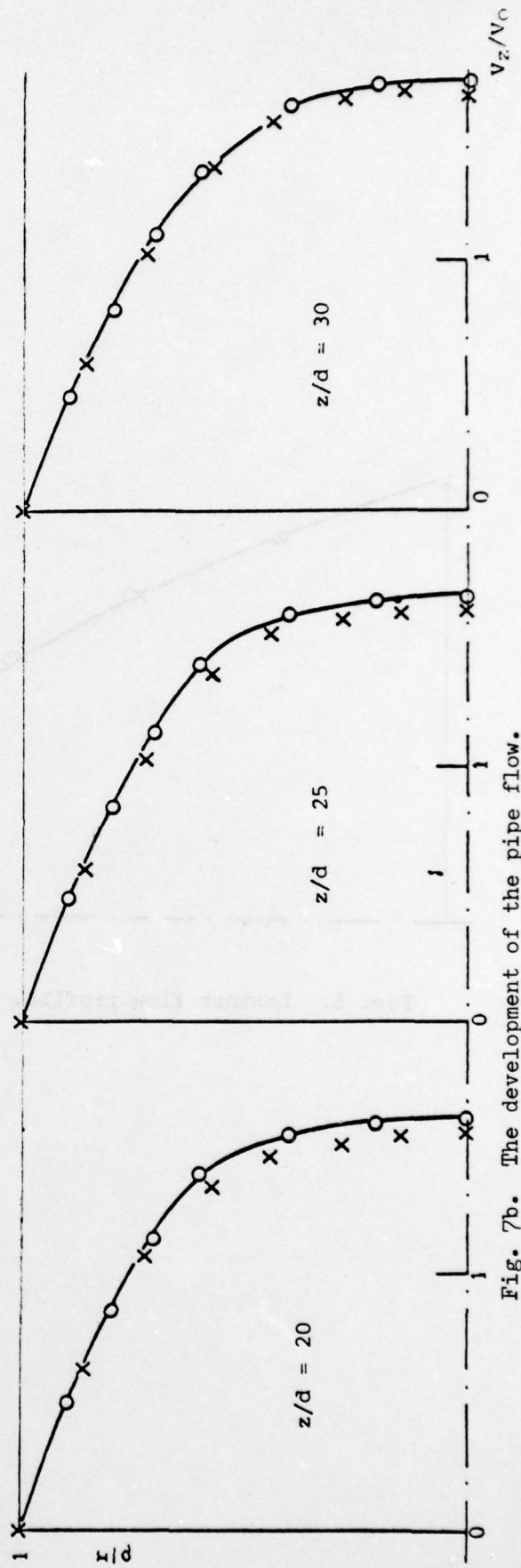


Fig. 7b. The development of the pipe flow.

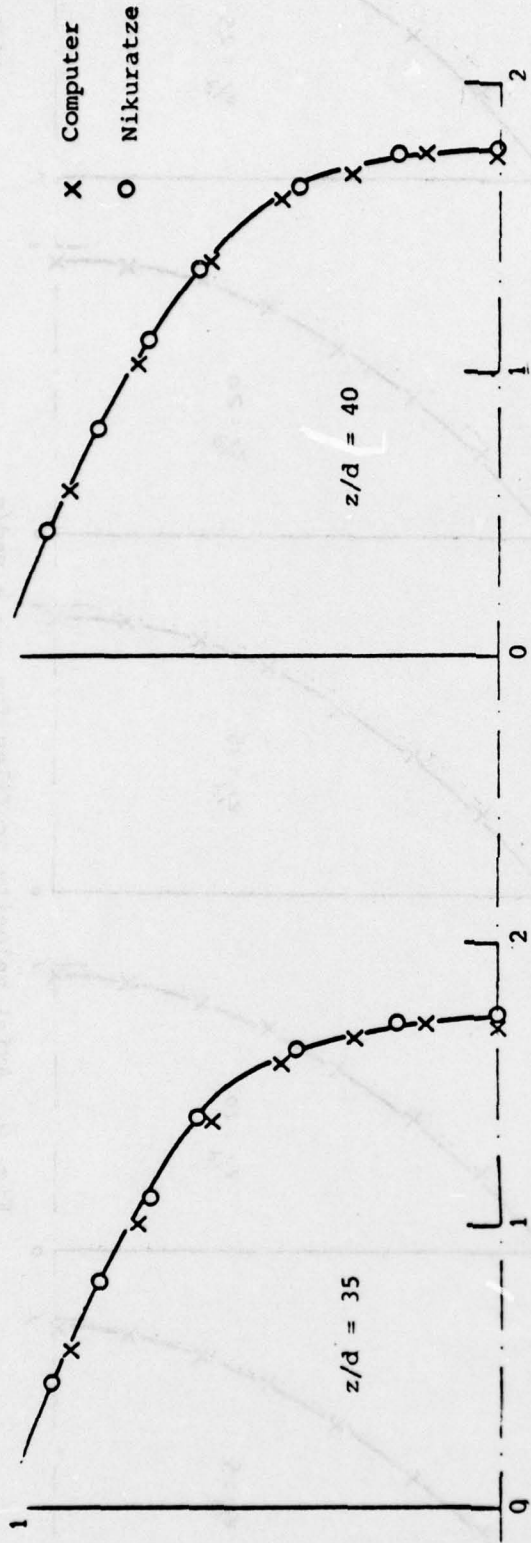


Fig. 7c. The development of the pipe flow.

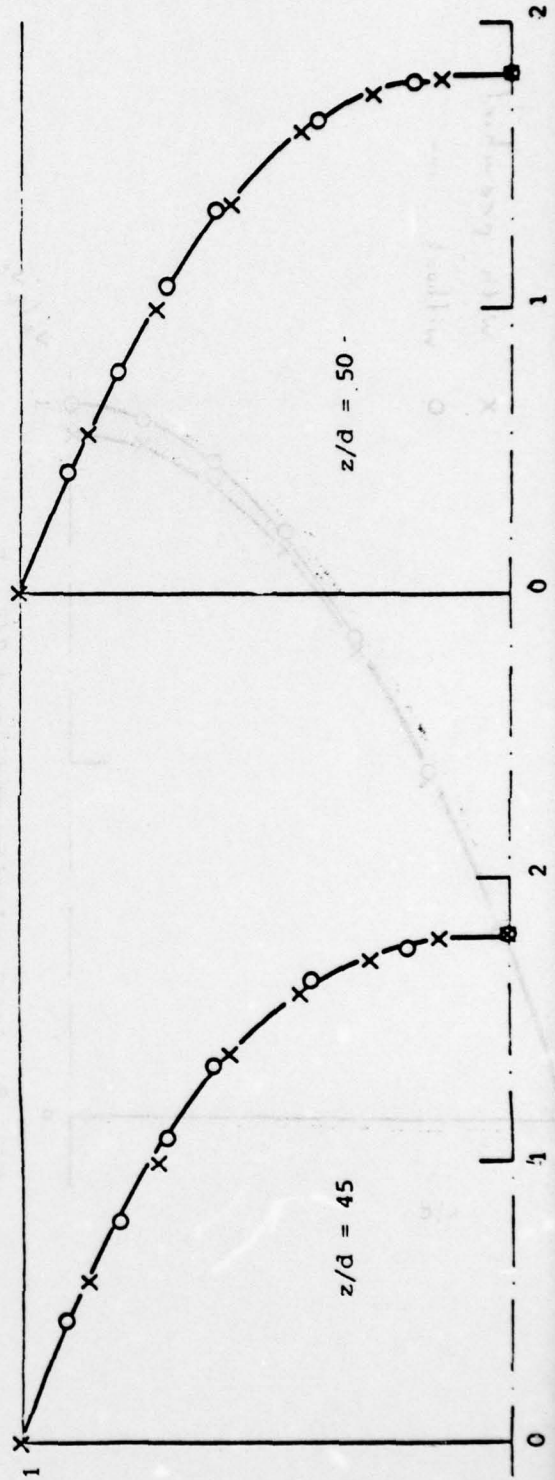


Fig. 7d. The development of the pipe flow.

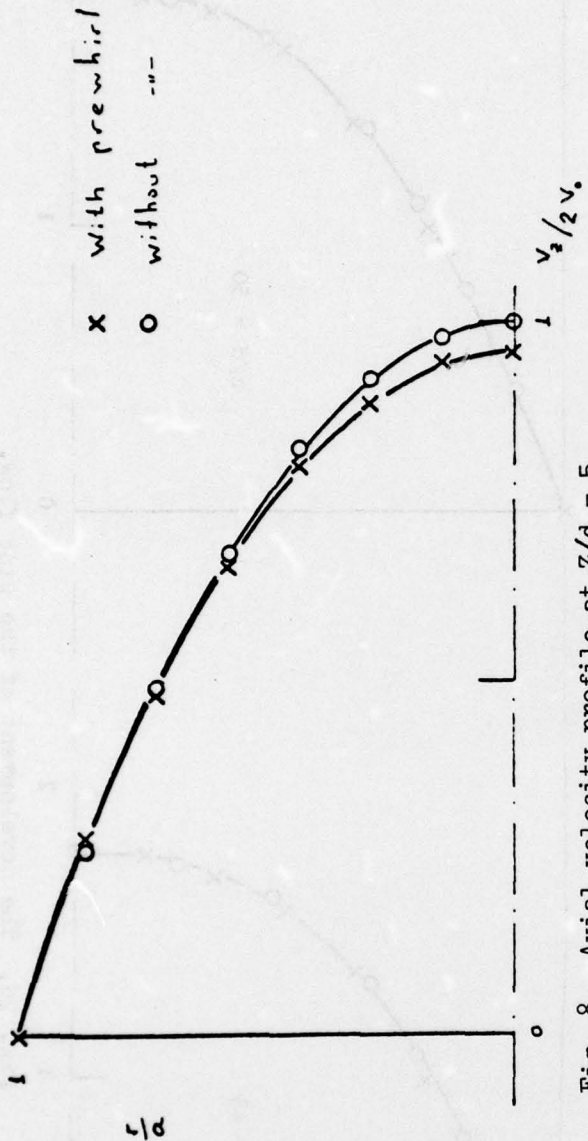


Fig. 8. Axial velocity profile at  $Z/d = 5$

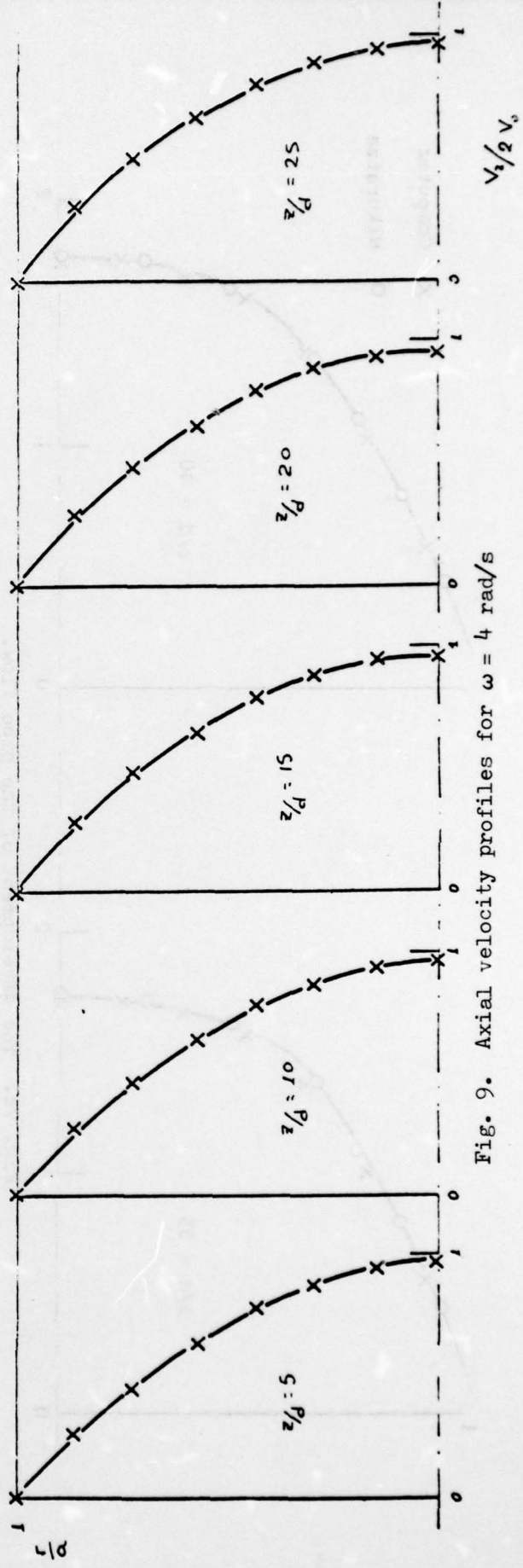


Fig. 9. Axial velocity profiles for  $\omega = 4$  rad/s

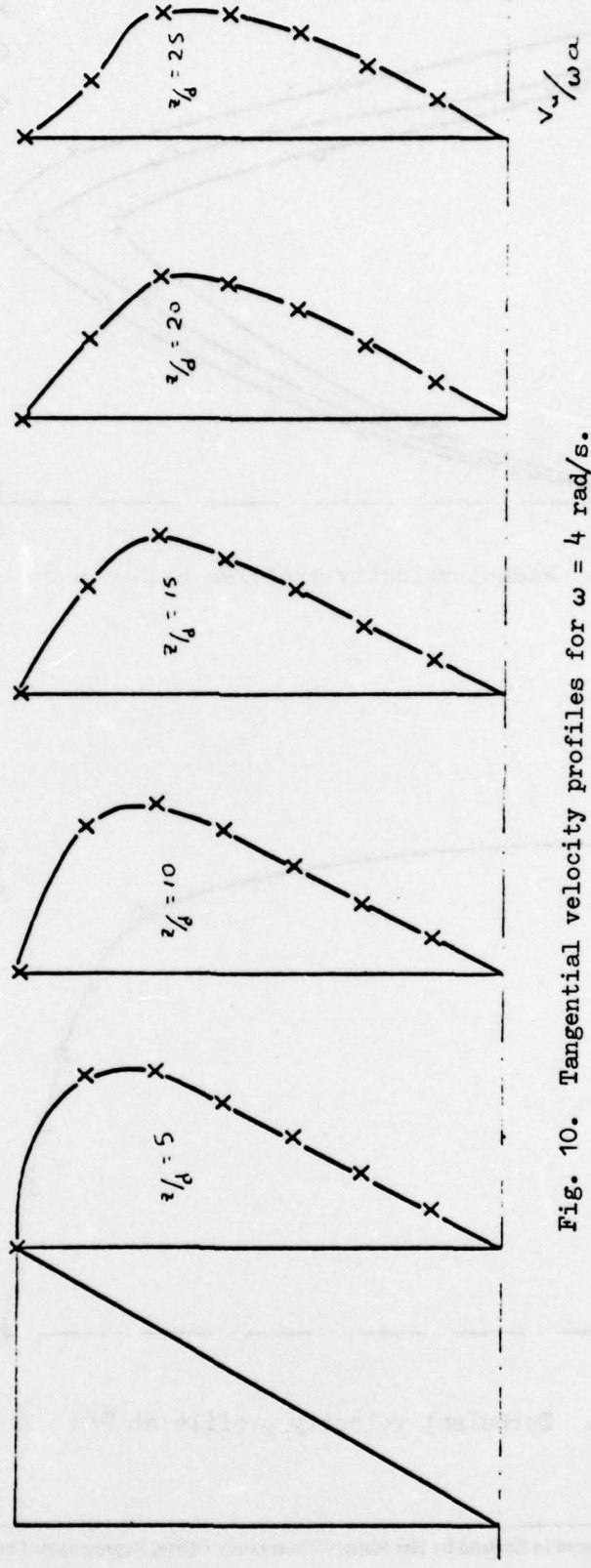


Fig. 10. Tangential velocity profiles for  $\omega = 4$  rad/s.



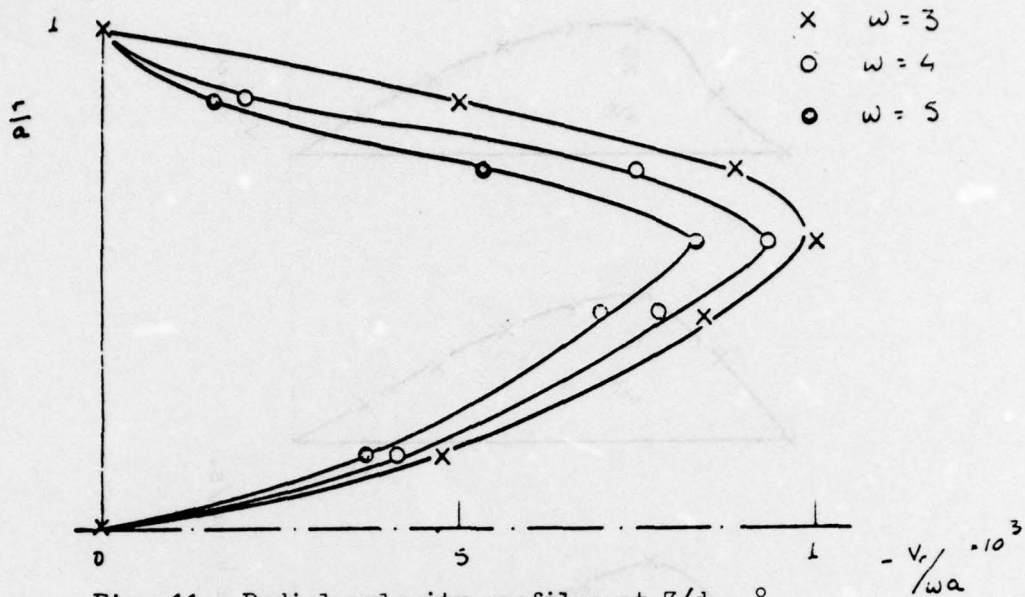


Fig. 11. Radial velocity profiles at  $Z/d = 8$

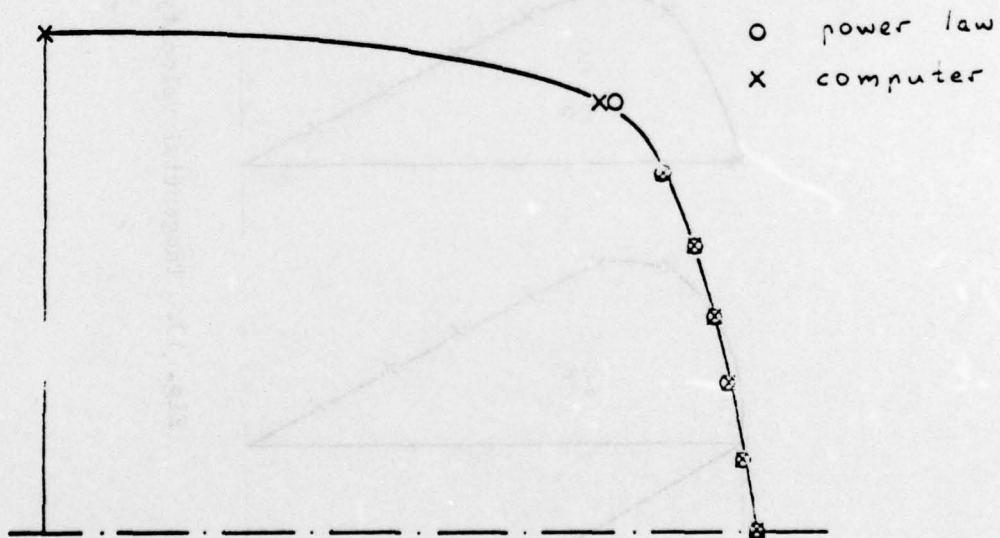


Fig. 12. Turbulent velocity profile at  $Z/d = 6$

A.R.C. CP No. 1382  
November 1976  
Goulas, Apostolos and Baker, Roger C.

THROUGH FLOW ANALYSIS OF  
VISCIOUS AND TURBULENT FLOWS

The matrix through-flow analysis is extended to cover turbulent and viscous flows by solving the streamwise equation of motion to obtain a suitable entropy field derived from the stresses.

The results of computation for straight circular pipe flows agree well with published data for laminar flow with and without swirl and for turbulent flow.

A.R.C. CP No. 1382  
November 1976  
Goulas, Apostolos and Baker, Roger C.

THROUGH FLOW ANALYSIS OF  
VISCIOUS AND TURBULENT FLOWS

The matrix through-flow analysis is extended to cover turbulent and viscous flows by solving the streamwise equation of motion to obtain a suitable entropy field derived from the stresses.

The results of computation for straight circular pipe flows agree well with published data for laminar flow with and without swirl and for turbulent flow.

A.R.C. CP No. 1382  
November 1976  
Goulas, Apostolos and Baker, Roger C.

THROUGH FLOW ANALYSIS OF  
VISCIOUS AND TURBULENT FLOWS

The matrix through-flow analysis is extended to cover turbulent and viscous flows by solving the streamwise equation of motion to obtain a suitable entropy field derived from the stresses.

The results of computation for straight circular pipe flows agree well with published data for laminar flow with and without swirl and for turbulent flow.

A.R.C. CP No. 1382  
November 1976  
Goulas, Apostolos and Baker, Roger C.

THROUGH FLOW ANALYSIS OF  
VISCIOUS AND TURBULENT FLOWS

The matrix through-flow analysis is extended to cover turbulent and viscous flows by solving the streamwise equation of motion to obtain a suitable entropy field derived from the stresses.

The results of computation for straight circular pipe flows agree well with published data for laminar flow with and without swirl and for turbulent flow.